CHAPTER 4

CHAPTER 4

Elucidating the molecular interactions of selected secondary metabolites from *S. virginianum* leaf extracts: Insights from molecular docking and apoptotic marker analysis

4.1 Introduction

Molecular docking is a cornerstone technique in structural molecular biology and computer-assisted drug design, significantly shaping the contemporary landscape of drug development (Tiwari et al., 2024). This technique enables the anticipation of interactions between minute ligands and protein molecules, or even between two protein molecules, elucidating the binding modes responsible for protein inhibition (De Ruyck et al., 2016). Understanding these interactions at the molecular level is imperative for discerning the efficacy of the investigated molecule (Rai et al., 2023).

In silico methodologies offer a promising avenue for comprehending the potential therapeutic impacts of natural compounds or secondary metabolites derived from plant extracts on breast cancer cells (Shrihastini et al., 2021). Our recent investigation revealed that *Sv* leaf extracts exhibited significant anti-proliferative effects on MCF-7 and MDA-MB-231 cells when combined with melatonin (Chapter 4). To elucidate the active metabolites, present in these extracts, we conducted GC-MS and HR-LCMS/MS analyses (Chapter 3). This chapter encompasses the determination of binding affinities of selected secondary metabolites identified through advanced analytical methods and an exploration of apoptotic and cell cycle markers.

4.2 Materials and method

4.2.1 Ligand preparation

The structures of selected phyto-compounds were acquired from the PubChem database (https://pubchem.ncbi.nlm.nih.gov/) in Structured Data File (SDF) format. Subsequently, these

files were converted into Protein Data Bank (PDB) format using the Online Smile Translator (https://cactus.nci.nih.gov/translate/).

4.2.2 Drug Likeliness Prediction of ligand

4.2.2.1 Lipinski Rule of '5' Analysis

According to the "rule of five" by Lipinski, a suitable option for an orally active medication is one that does not exceed one deviation from the following guidelines: <5 hydrogen bond donors, <10 hydrogen bond acceptors, molecular weight < 500, log P < 5. Subsequently, the "prepare ligands" module was employed on the remaining compounds to produce various conformations.

4.2.2.2 ADME/T Properties Analysis

To assess the pharmacokinetic characteristics and potential toxicity of the selected phytocompounds, computational models evaluating ADME (Absorption, Distribution, Metabolism, Excretion) were employed. These models aid in identifying molecules with favourable drug-like properties for further development. The parameters chosen for analysis encompassed intestinal absorption (in human % absorption), blood-brain barrier permeability, CYP2D6 substrate, CYP2D6 inhibitor, total clearance, AMES toxicity, oral rat acute toxicity, oral rat chronic toxicity, and hepatotoxicity. This comprehensive evaluation provides insights crucial for determining the suitability of these compounds for therapeutic applications.

4.2.2.3 Protein preparation

The three-dimensional crystal structures of cell cycle proteins [Cyclin D1 (PDB id: 2w99_A); Cyclin D3 (PDB id: 2w99_B); CDK4 (PDB id: 3g33_A); CDK6 (PDB id: 1g3n_A); P18 (PDB id: 1g3n_B); p21 (PDB id: 1axc_B); p27 (PDB id: 1jsu_C)] and apoptotic proteins [BAX (PDB id: 2k7w_B); BAK (PDB id: 2yv6_A); Bcl-2 (PDB id: 1g5m_A); Bcl-XL (PDB id: 1g5j_A); caspase-3 (PDB id: 1gfw_A); caspase-9 (PDB id: 1nw9_B)] were retrieved from the Protein Data Bank. The AutoDock Tools within the PyRx software version 0.8 were employed to prepare the protein structures. Initial structures were cleaned by removing water molecules and non-standard residues.

Subsequently, all missing hydrogens and Kollman charges were added to the system. The prepared target proteins were then saved in PDBQT file format.

4.2.3 Molecular Docking

Docking investigations were conducted utilizing the previously prepared target macromolecules and natural compounds employing PyRx software version 0.8. The aim of docking was to ascertain a population of potential conformations and orientations for the ligand within the protein's binding site. The protein was loaded into PyRx software 0.8, resulting in a PDBQT file with a protein structure containing hydrogens in all polar residues. All ligand bonds were rendered rotatable. The Lamarckian Genetic Algorithm (LGA) approach was employed for all computations, maintaining the protein-fixed ligand-flexible docking paradigm.

The docking location on the protein target was delineated by generating a grid box with a default grid spacing value. The lowest binding energy (BE, kcal/mol) and root mean square deviation (RMSD) conformation were optimal docking positions. Throughout the in silico experiment, an exhaustiveness of ten was selected for docking, and the number of modes was set at ten to ensure more accurate and reliable results. The interaction between ligands and proteins was established, visualized, and evaluated using BIOVIA Discovery Studio 4.1 visualizer (Pon Nivedha et al., 2017).

4.3 Result

Advanced analytical techniques identified more than 30 secondary metabolites in *Sv* leaf extracts (Chapter 5). Among these, Ritterazine A, Koryoginesenoside R1, Caffeoyl quinic acid, Aconine, Fabianine, Myricitrin, Pedalin, Quinic acid, and Sulfamethopyrazine were selected for molecular docking analysis with different receptors involved in apoptotic and cell cycle pathways. The chosen targets and their respective PDB IDs are provided in Table 4.3.3.

Previously, these nine selected phytocompounds had not been studied for anti-cancer pathway investigations through molecular docking. By docking the phytochemicals to the active

sites of the target proteins, their action was potentially enhanced. Furthermore, adherence to the Lipinski rule of five in our study suggests that the identified phytocompounds are non-toxic to humans (Table 4.3.1).

Observations were made regarding the binding affinity, various types of bonding, particularly hydrogen bonds, and the interaction of amino acid residues with the ligand and the bond length between the ligand atom and the target protein (Table 4.3.3 and 4.3.4). The binding affinities of the target proteins for all phytocompounds (ligands) were determined in terms of kcal/mol. Additionally, the observations revealed many hydrogen bonds and non-bonded interactions with all the target proteins. Hydrogen bonds suggest a high affinity for binding between the ligand and the protein. In contrast, a high negative score indicates a strong affinity for binding of the target protein.

In the present study, the residual interactions revealed the amino acids of the proteins the ligands bind to. All the identified compounds demonstrated robust affinity with the target proteins in terms of binding energy. Of the nine compounds docked, Ritterazine A exhibited strong binding with all the selected target proteins (Figure 4.3.1to 4.3.4). It displayed binding energies above 9 kcal/mol with all the target proteins, and the amino acid Glu-255 formed a strong binding interaction with Cyclin-D1. Cyclin-D3 interacted with Ritterazine A through the amino acids GLN-182 and PHE-287. The amino acid residues ASP-144, GLU-228, and ALA-167 of CDK4 formed strong bindings with Ritterazine A. Similarly, CDK6 formed a strong hydrogen bond interaction with Ritterazine A through the amino acid residues PHE-39 and HIS -100, and it also formed a Pi-anion interaction with GLU-99. p18 and Ritterazine A interacted through the ARG-79. p21 exhibited unfavourable interaction with the residue LEU-157. p27 formed a strong hydrogen bond interaction with Ritterazine A through LYS-81 and TYR-88 and a Pi-Alkyl interaction with residue TRP-76. BAX and Ritterazine A formed only one interaction with TYR-162. Similarly, BAK and Ritterazine A formed only one hydrogen bond interaction through GLN-94. The target Bcl-2 formed one hydrogen bond and one Pi-Anion interaction through the residues SER-49 and ASP-10,

respectively. Bcl-xl and Ritterazine A formed a pi-alkyl interaction through ARG-104. Caspase-3 and Ritterazine A did not form a significant interaction but exhibited very good binding energy. Caspase-3 and Ritterazine A demonstrated strong binding through a hydrogen bond and pi-alkyl interaction with the residues LYS-410 and LEU-145, respectively. These interactions confirm that Ritterazine A exhibits good activity against all selected target proteins. Hence, suggesting a slight modification in its structure while retaining the pharmacophore feature would be a better approach to retain this molecule as a potential drug candidate.

Table 4.3.1: ADME/T analysis of selected secondary metabolites

Compound name	Intestinal absorption (human) (% Absorbed)	BBB permeability (log BB)	CYP2D6 substrate (Yes/No)	CYP2D6 inhibitor	Total Clearance (log ml/min/kg)	AMES toxicity (Yes/No)	Oral Rat Acute Toxicity (LD50) (mol/kg)	Oral Rat Chronic Toxicity (LOAEL) (log mg/kg_bw/day)	Hepatotoxicity (Yes/No)
Aconine	64.628	-1.273	No	No	0.05	Yes	2.607	2.991	No
Fabianine	94.094	0.32	No	No	1.013	No	2.239	1.708	No
Koryogenoside R1	31.722	-1.888	No	No	0.468	No	3.313	2.876	No
Myricitrin	43.334	-1.811	No	No	0.303	No	2.537	3.386	No
Pedaliin	38.429	-2.017	No	No	0.42	No	2.565	4.339	No
Caffeoyl quinic acid	35.560	-2.598	No	No	0.45	No	2.563	3.589	No
Quinic acid	32.274	-2.737	No	No	0.639	No	1.128	3.529	No
Ritterazine A	100.000	-0.987	No	No	-1.57	No	3.523	2.104	Yes
Sulfamethopyrazine	79.093	-0.077	No	No	0.643	No	2.000	1.935	Yes

Table 4.3.2: Binding energy of selected compounds						
Compound name	**Molecular weight**	**Log P**	**Rotatable bonds**	**Acceptors**	**Donors**	**Surface area**
Aconine	499.601	-1.7874	6	10	5	205.648
Fabianine	219.328	3.141182	1	2	1	97.724
Koryogenoside R1	869.099	2.2468	12	15	9	360.625
Myricitrin	464.379	0.1943	3	12	8	183.901
Pedaliin	478.406	-0.2359	5	12	7	190.586
Caffeoyl quinic acid	354.308	-0.2894	4	5	7	154.23
Quinic acid	192.167	-2.3214	1	5	5	74.056
Ritterazine A	913.206	4.7269	0	12	5	389.945
Sulfamethopyrazine	280.309	0.8682	4	6	2	110.057

Table 4.3.3: PDB ID of selected target proteins	
Cell cycle proteins	**PDB ID with Chain**
Cylcin D1	2w99_A
Cyclin D3	2w99_B
CDK4	3g33_A
CDK6	1g3n_A
P18	1g3n_B
p21	1axc_B
p27	1jsu_C

Table 4.3.4: Target-Ligand interaction score													
		Target											
S.no	**Ligands**	**Cyclin D1**	**CDK 6**	**Cyclin D3**	**CDK4**	**p18**	**p21**	**p27**	**Bax**	**Bak**	**BCL2**	**BCL-XL**	**Caspase3**	**Caspase9**
1	Ritterazine A	-9.6	-10.8	-9.5	-9.9	-9.5	-7.1	-10.3	-6.3	-10.3	-10.7	-10.4	-9	-11.4
2	Koryoginesenoside R1	-7.6	-8	-8.3	-7.7	-7.3	-5.7	-7.5	-5.3	-8.8	-7.2	-7.4	-6.1	-6.8
3	Caffeoyl quinic acid	-6.8	-7.5	-8.6	-7.5	-6.5	-4.8	-5.8	-5.1	-7.2	-7.6	-6.8	-6.2	-6.6
4	Aconine	-6.5	-6.1	-6.1	-6.3	-5.5	-4.3	-5.3	-4.2	-7.2	-6.4	-6	-5.4	-5.4
5	Fabianine	-6.2	-7	-7.1	-5.6	-5.7	-4.2	-5.3	-4.5	-6.3	-6	-6.8	-5.7	-5.9
6	Myricitrin	-7.5	-7.6	-9.8	-8.3	-7.4	-5.8	-6.1	-5.3	-7.7	-8.3	-7	-6.3	-7.2
7	Pedalin	-7.2	-8.5	-8.7	-8.2	-7	-5.4	-6.1	-5.6	-7.7	-7.9	-8	-6.5	-7.4
8	Quinic acid	-5.3	-5.6	-6.5	-6	-5	-3.9	-4.7	-3.8	-5.7	-5.5	-5.8	-4.6	-5.9
9	Sulfamethopyrazine	-6.1	-6.9	-7.3	-6.9	-5.5	-4.7	-5	-4.7	-6.5	-6.2	-6	-5.3	-6.3

**The rmsd/ub and rmsd/ld for all selected compounds were considered 0 where as rmsd/ub : Root Mean Square Deviation upper bound and rmsd/lb : Root Mean Square Deviation lower bound*

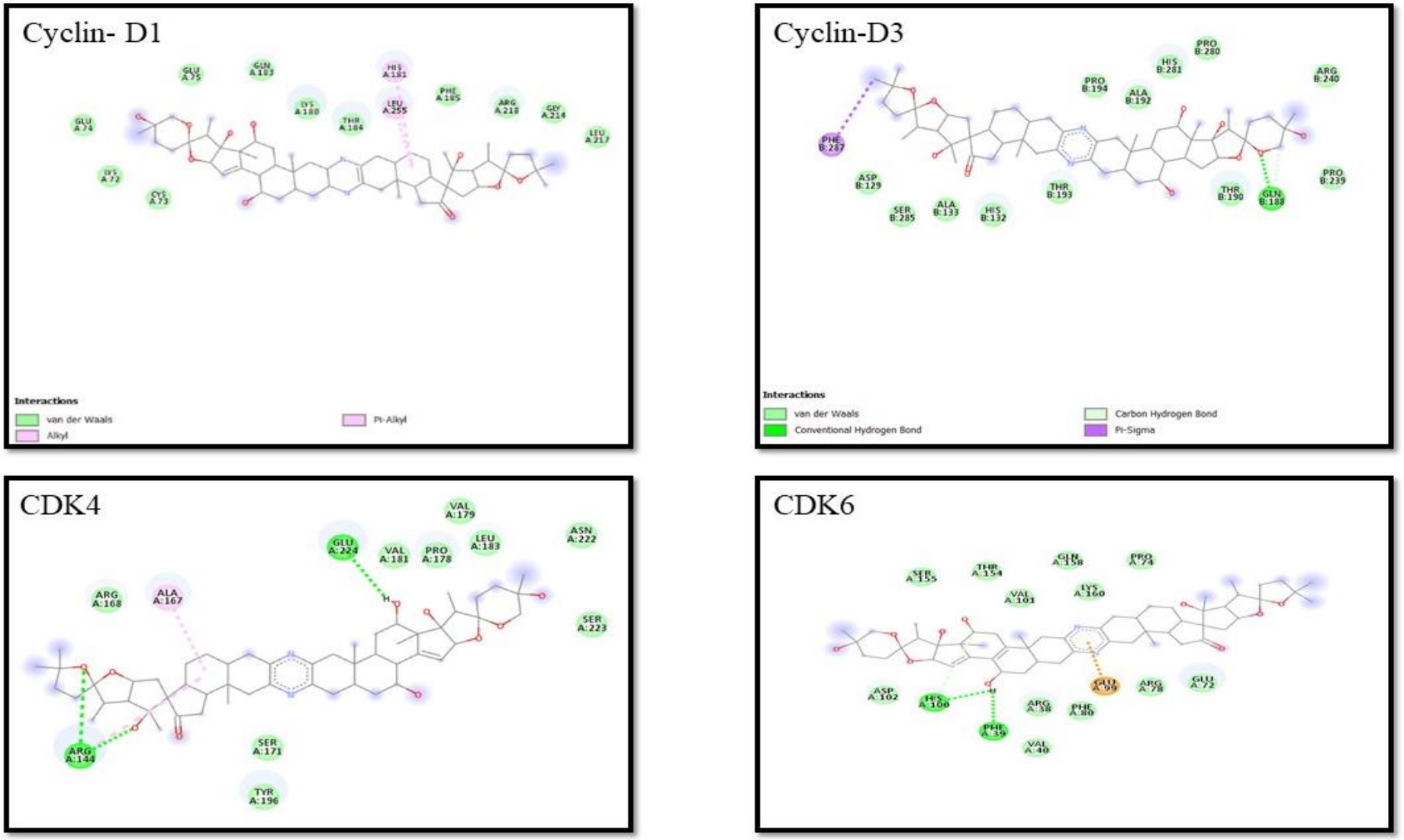

Figure 4.3.1: Images represents the interaction between Target Cyclin D1, Cyclin-D4, CDK4 and CDK6 with ligand Ritterazine A.

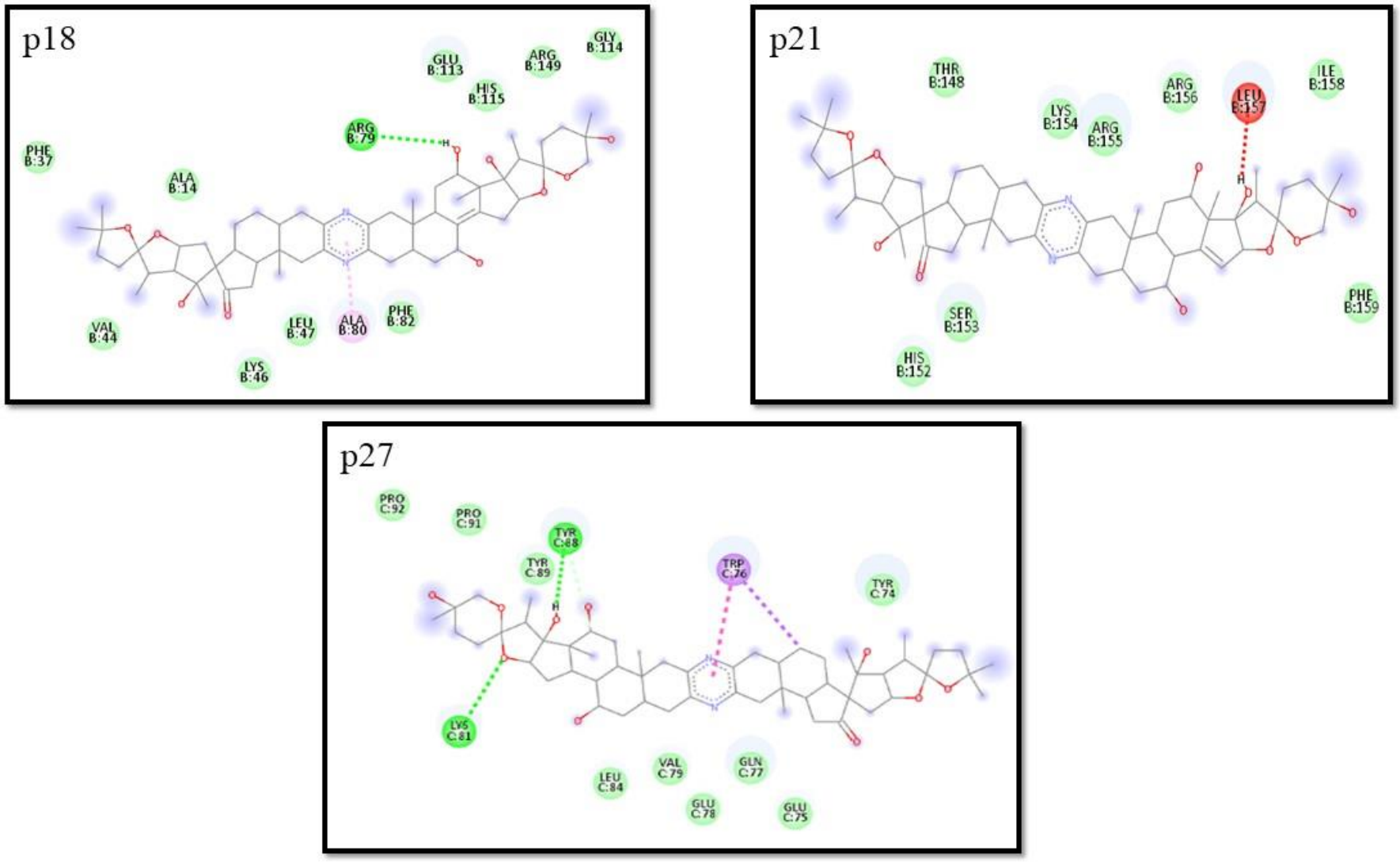

Figure 4.3.2: Images represents the interaction between Target p18, p21 and p27with ligand Ritterazine A.

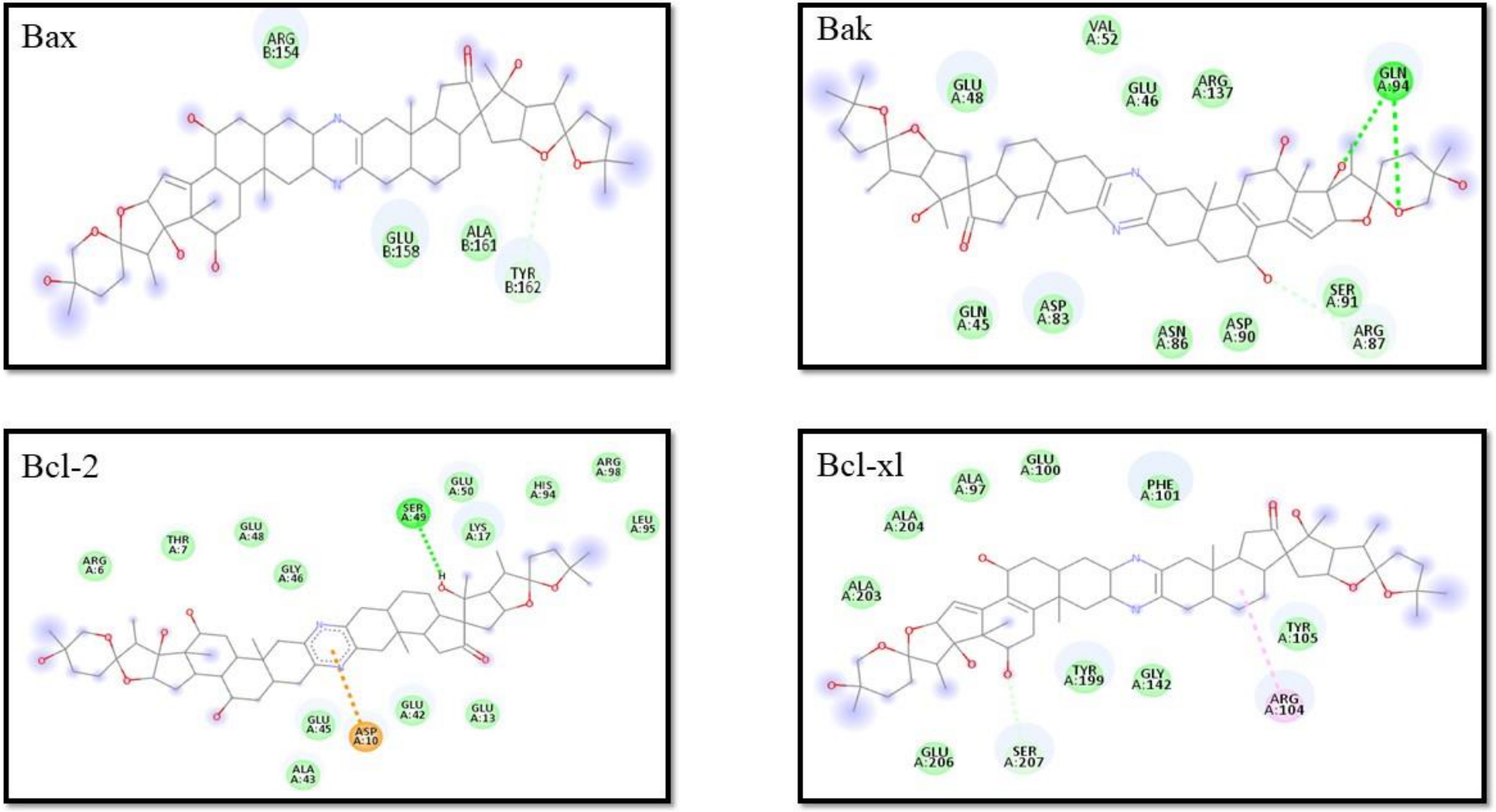

Figure 4.3.3: Images represents the interaction between Target Bax, Bak, Bcl-2 and Bcl-xl with ligand Ritterazine A.

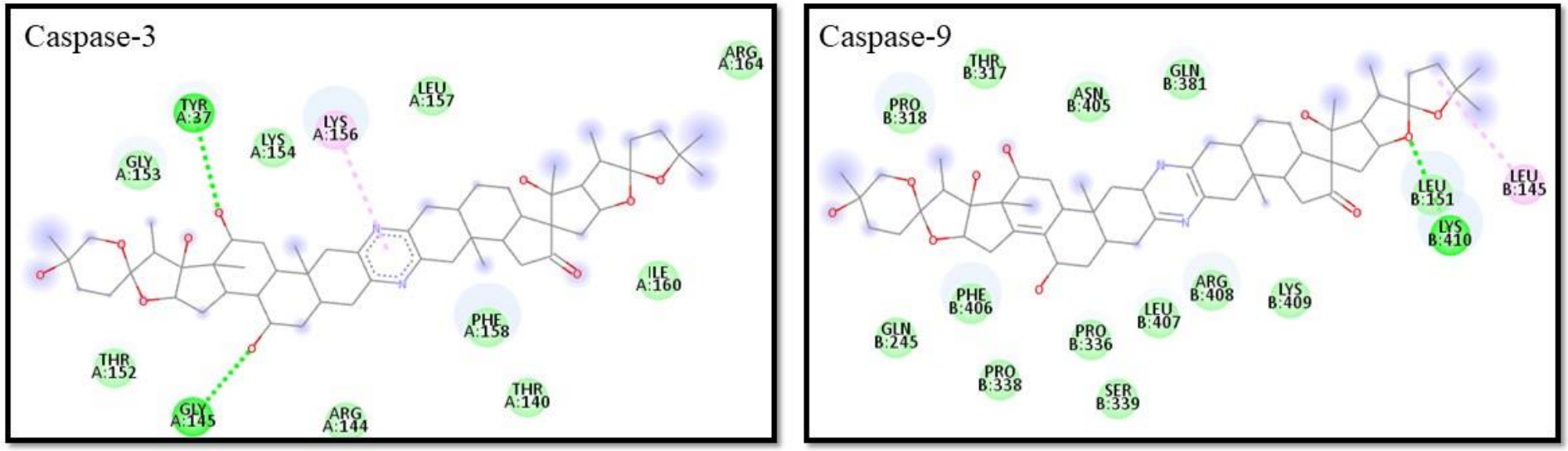

Figure 4.3.4: Images represents the interaction between Target caspase-3 and caspase-9 with ligand Ritterazine A.

4.4 Discussion

The significance of natural products in developing anticancer and antioxidant-based lead compounds for cancer treatment is increasingly recognized. While computational algorithm methods are well-documented in synthetic medicinal chemistry, their utilization in natural phytocompounds remains underexplored (Romano et al.,2019). Molecular docking serves the purpose of predicting the structure of ligand-receptor complexes through computational means. This method facilitates the virtual screening of a compound library, with the results ranked based on scores. It aids in formulating structural hypotheses regarding how ligands inhibit target receptors, which is crucial for lead optimization. Docking is influenced by various intramolecular and intermolecular forces, including bond width, bond angle, dihedral angle, electrostatic interactions, dipolar interactions, hydrogen bonding, and hydrophobicity (Pissurlenkar et al.,2009).

Previously, steroidal alkaloids (such as Solanidine, Solasodine, alpha-Solanine, and Solasonine) from Solanum nigrum were subjected to molecular docking analysis with different cytoskeletal proteins (Ahmad,2019). This study marks the first assessment of nine specific phyto-compounds through molecular docking experiments. The comprehensive *in-silico* investigation reveals that Ritterazin A exhibits a favourable binding affinity towards selected cancer sites, positioning it as a potential candidate for future breast cancer therapies. The *in-silico* findings substantiate the anti-proliferative effects of *Sv* leaf extracts on MCF-7 and MDA-MB-231 cell lines. Subsequent chapters delve into apoptotic activity via *in-vitro* tests and molecular research. Numerous docking analyses for specific phytocompounds and melatonin could be pursued.

The overall in silico studies presented in this chapter were performed at DBT-BIF Centre, Holy Cross College (Autonomous), Tiruchirappalli, Tamil Nadu under the guidance and collaboration with* ***Dr. RAJALAKSHMI M.* *Assistant Professor in Biotechnology. Department of Zoology, Head, PG & Research Department of Biotechnology & Bioinformatics.*